

# The Analytical Theory of Bulk Melting I: Exact Solution of the One-dimensional Atom Chain

Yajun Zhou † and Xiaofeng Jin ‡

*Surface Physics Laboratory & Department of Physics, Fudan University, Shanghai 200433, China*

(Dated: October 5, 2018)

We investigate theoretically the crucial rôle of interstitialcies that trigger the melting of a boundary-free crystal. Based on an interstitialcy model that resembles the  $J_1$ - $J_2$  model of frustrated antiferromagnets with uniaxial anisotropy, we have calculated the exact partition function and correlation functions in a one-dimensional atom chain. The melting point and correlation behavior of this crystal model show the applicability of Lindemann criterion and Born criterion in the one-dimensional case.

PACS numbers: 64.70.Dv, 64.60.Qb

## I. INTRODUCTION

The physical picture of solid-liquid phase transition has emerged as a controversial issue motivated by both science and industry since early 20th century when divergent accounts of the instability mechanism and atom-scale pathway towards melting in various theoretical models did not seem to yield a unanimous prediction for the melting point of a realistic system<sup>1,2,3,4,5,6,7</sup>. The widely-cited Lindemann<sup>1</sup> and Born<sup>2</sup> criteria, do not form an exception to this discrepancy at a glance: in the former criterion, Lindemann proposed that melting is triggered by the avalanche of the root-mean-square atom displacement as soon as it exceeds a threshold fraction ( $\delta_L^*$ ) of the atom spacing, where  $\delta_L^*$  is called the critical Lindemann ratio, a semi-empirical parameter initially conceived as a lattice type characteristic (but experiments<sup>8</sup> suggest otherwise); in the latter criterion, Born argued that the vanishment of shear modulus (Ref.<sup>9</sup> challenges this vanishment experimentally) is responsible for the inability to resist lattice destruction at the melting point.

In this series of papers, we give a detailed presentation of how to join the Lindemann and Born criteria together. We use a model analogous to the  $J_1$ - $J_2$  model for frustrated antiferromagnets to formulate that the cooperative creation and the spatial correlation of interstitialcies are the impetus that triggers and propagates instability in a crystal and that eventually undermines long-range order in the surface-free solid (bulk material). This idea is inspired by a recent molecular dynamics simulation in which the rôle of interstitialcies is emphasized<sup>10</sup>, the previous understandings of the rôles of vacancies in surface melting<sup>11</sup>, the formation and motion of interstitial clusters in metals<sup>12,13,14,15</sup> and semiconductors<sup>16,17,18</sup>, early theories of interstitialcies based on computer simulations<sup>19,20</sup> and some thermodynamic arguments<sup>21,22</sup>, and especially the notion of “virtual attraction” between defects in Ref.<sup>20</sup>.

This paper deals with the exact solution of the boundary-free one-dimensional (1D) atom chain where two independent analytical algorithms are applied to evaluate the partition function. Sect. II presents a brief

account of the methodology of our interstitialcy model; Sect. III provides an exact solution to the model based on the transfer matrix; Sect. IV is the summary of the results in Paper I; Appendix A elaborates on a solution to our model through Kac-Ward method, which serves as a valuable check to the results in Sect. III.

## II. MODEL HAMILTONIAN

We begin our argument with the Hamiltonian of a 1D atom chain composed of  $N$  atoms and  $2N$  sites (See FIG. 1 for the site labelling):

$$\mathcal{H}_{\text{conf}} = \sum_{k=1}^{2N} (J_1 n_k n_{k+1} + J_2 n_k n_{k+2}), \quad (1)$$

where the Boolean variable  $n_k$  is the number of atoms occupying site  $k$ .  $n_k = 0$  or  $1$ . In this paper, we assume  $J_1 > 0$  and  $J_2 < 0$  unless specified. In this Hamiltonian, the potential energy is set to be  $J_1$  for each nearest-neighbor (NN) atom pair,  $J_2$  for each next-nearest-neighbor (NNN) atom pair and zero otherwise. In order to adapt to the question under investigation, we need two restrictions

$$n_{k+2N} = n_k, \quad \sum_{k=1}^{2N} n_k = N \quad (2)$$

to reflect the periodical boundary condition and atom number conservation respectively. By using the transformation<sup>23,24,25</sup>  $\sigma_k = 2n_k - 1$ , one could map the Hamiltonian above to the  $J_1$ - $J_2$  model<sup>26</sup> of a 1D frustrated antiferromagnet

$$\mathcal{H}_{\text{conf}} = \frac{1}{4} \sum_{k=1}^{2N} (J_1 \sigma_k \sigma_{k+1} + J_2 \sigma_k \sigma_{k+2}) + \text{const}, \quad (3)$$

where  $\sigma_k = \sigma_{k+2N} = \pm 1$ , and  $\sum_{k=1}^{2N} \sigma_k = 0$ . When  $T = 0\text{K}$ , sites labeled by an odd (or even) number  $k$  are all occupied by atoms. In the light of this, we may call the odd-number sites as lattice sites and call the even-number sites as interstitialcy sites, as shown in FIG. 1,

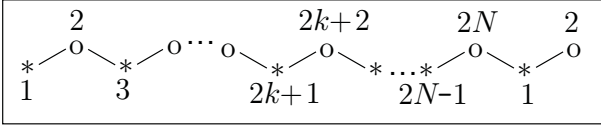


FIG. 1: The way we label the lattice sites “\*” and interstitial sites “o” in 1D atom chain.

or vice versa. The lattice sites and interstitial sites interpenetrate.

### III. THE TRANSFER MATRIX APPROACH

#### A. The Partition Function for $T > 0\text{K}$ and Thermodynamic Properties

To lift the constraint  $\sum_{k=1}^{2N} \sigma_k = 0$ , we introduce a phenomenological external field  $h$  and consider the following Hamiltonian:

$$\mathcal{H}(\sigma, h) = h \sum_{k=1}^{2N} \sigma_k + \frac{1}{4} \sum_{k=1}^{2N} (J_1 \sigma_k \sigma_{k+1} + J_2 \sigma_k \sigma_{k+2}) \quad (4)$$

with the condition  $\sigma_{k+2N} = \sigma_k$ . If one could (i) evaluate the canonical partition function corresponding to  $\mathcal{H}(\sigma, 0)$  for any absolute temperature  $T > 0\text{K}$  (to be elaborated in this subsection):

$$Q_N = \text{Tr} e^{-\mathcal{H}(\sigma, 0)/k_B T} = \sum_{\{\sigma_k = \pm 1\}} e^{-\mathcal{H}(\sigma, 0)/k_B T} \quad (5)$$

( $k_B$ : Boltzmann constant); and (ii) could show that the “ensemble average”

$$\begin{aligned} & \left\langle \frac{1}{N} \sum_{k=1}^{2N} \sigma_k \right\rangle_{\mathcal{H}(\sigma, 0)} \\ &= \frac{1}{N} \frac{\partial}{\partial h} \text{Tr} e^{-\mathcal{H}(\sigma, h)/k_B T} \Big|_{h=0} \\ &= \text{Tr} \left[ \left( \frac{1}{N} \sum_{k=1}^{2N} \sigma_k \right) e^{-\mathcal{H}(\sigma, 0)/k_B T} \right] \end{aligned} \quad (6)$$

vanishes in the thermodynamic limit  $N \rightarrow \infty$  (to be elaborated in the next subsection), then it will be safe to say that  $Q_N = \text{Tr} e^{-\mathcal{H}(\sigma, 0)/k_B T}$  is also the exact partition function corresponding to the Hamiltonian  $\mathcal{H}_{\text{conf}}$  in the thermodynamic limit because  $\left\langle \frac{1}{N} \sum_{k=1}^{2N} \sigma_k \right\rangle_{\mathcal{H}_{\text{conf}}} \equiv 0$ .

In order to evaluate  $Q_N = \text{Tr} e^{-\mathcal{H}(\sigma, 0)/k_B T}$ , we need to construct a  $4 \times 4$  transfer matrix  $\hat{T} = (\hat{T}_{\Sigma \Sigma'})$  so that<sup>27,28</sup>

$$\begin{aligned} Q_N &= \sum_{(\sigma)} \exp \left[ -\frac{1}{4k_B T} \sum_{k=1}^{2N} (J_1 \sigma_k \sigma_{k+1} + J_2 \sigma_k \sigma_{k+2}) \right] \\ &= \sum_{(\sigma)} \hat{T}_{\Sigma_1 \Sigma_2} \hat{T}_{\Sigma_2 \Sigma_3} \cdots \hat{T}_{\Sigma_{N-1} \Sigma_N} = \text{Tr} \hat{T}^N \end{aligned} \quad (7)$$

where  $\Sigma_k = \sigma_{2k-1} + i\sigma_{2k}$ . Such a transfer matrix must take the form:

$$\begin{aligned} \hat{T} &= \begin{bmatrix} \hat{T}_{-1-i, -1-i} & \hat{T}_{-1-i, -1+i} & \hat{T}_{-1-i, 1-i} & \hat{T}_{-1-i, 1+i} \\ \hat{T}_{-1+i, -1-i} & \hat{T}_{-1+i, -1+i} & \hat{T}_{-1+i, 1-i} & \hat{T}_{-1+i, 1+i} \\ \hat{T}_{1-i, -1-i} & \hat{T}_{1-i, -1+i} & \hat{T}_{1-i, 1-i} & \hat{T}_{1-i, 1+i} \\ \hat{T}_{1+i, -1-i} & \hat{T}_{1+i, -1+i} & \hat{T}_{1+i, 1-i} & \hat{T}_{1+i, 1+i} \end{bmatrix} \\ &= \begin{bmatrix} e^{-2\beta'(J_1+J_2)} & e^{-\beta'J_1} & e^{\beta'J_1} & e^{2\beta'J_2} \\ e^{\beta'J_1} & e^{2\beta'(J_1-J_2)} & e^{2\beta'J_2} & e^{-\beta'J_1} \\ e^{-\beta'J_1} & e^{2\beta'J_2} & e^{2\beta'(J_1-J_2)} & e^{\beta'J_1} \\ e^{2\beta'J_2} & e^{\beta'J_1} & e^{-\beta'J_1} & e^{-2\beta'(J_1+J_2)} \end{bmatrix} \\ &= \begin{bmatrix} \frac{(1-x_1)(1-x_2)}{(1+x_1)(1+x_2)} & \sqrt{\frac{1-x_1}{1+x_1}} & \sqrt{\frac{1+x_1}{1-x_1}} & \frac{1+x_2}{1-x_2} \\ \sqrt{\frac{1+x_1}{1-x_1}} & \frac{(1+x_1)(1-x_2)}{(1-x_1)(1+x_2)} & \frac{1+x_2}{1-x_2} & \sqrt{\frac{1-x_1}{1+x_1}} \\ \sqrt{\frac{1-x_1}{1+x_1}} & \frac{1+x_2}{1-x_2} & \frac{(1+x_1)(1-x_2)}{(1-x_1)(1+x_2)} & \sqrt{\frac{1+x_1}{1-x_1}} \\ \frac{1+x_2}{1-x_2} & \sqrt{\frac{1+x_1}{1-x_1}} & \sqrt{\frac{1-x_1}{1+x_1}} & \frac{(1-x_1)(1-x_2)}{(1+x_1)(1+x_2)} \end{bmatrix} \end{aligned} \quad (8)$$

where  $\beta' = (4k_B T)^{-1}$  and  $x_1 = \tanh \beta' J_1$ ,  $x_2 = \tanh \beta' J_2$ . The matrix elements are obtained like the following example:

$$\begin{aligned} \hat{T}_{1-i, -1+i} &= \exp \left\{ -\beta' \left( \begin{array}{cc} 2k & 2k+2 \\ \diagdown & \diagup \\ 1 & -1 \\ \diagup & \diagdown \\ 2k-1 & 2k+1 \end{array} \right) \right\} = \exp \left\{ -\beta' \left( \begin{array}{cc} & J_2 \\ \diagdown & \diagup \\ J_1/2 & -1 \\ \diagup & \diagdown \\ & J_2 \end{array} \right) \right\} \\ &= \exp \left\{ -\beta' \left[ (-1) \times (1) \frac{J_1}{2} + (-1) \times (1) J_2 + (-1) \times (-1) \frac{J_1}{2} + (-1) \times (1) J_2 + (-1) \times (1) \frac{J_1}{2} \right] \right\} \\ &= \exp (2\beta' J_2) \end{aligned} \quad (9)$$

Each interior interaction (thick black edges) energy in the cell diagram is counted as one, while each peripheral interaction (thin black edges) is counted as half because such “bonds” are shared by two cells.

The transfer matrix is diagonalized by  $\hat{T} = \hat{S}\hat{L}\hat{S}^{-1}$ ,

$$\lambda_1 = \frac{2 \left[ 1 + x_2^2 - 2x_2x_1^2 \mp (1-x_2) \sqrt{(1+x_2)^2 - 4x_2x_1^2} \right]}{(1-x_1^2)(1-x_2^2)}, \quad (10)$$

$$\lambda_3 = \frac{2 \left[ x_2(x_2x_1^2 - 2) + x_1^2 \mp (1-x_2) \sqrt{(1+x_2)^2 x_1^2 - 4x_2} \right]}{(1-x_1^2)(1-x_2^2)}. \quad (11)$$

In the thermodynamic limit, only the largest eigenvalue  $\lambda_2$  survives in the final expression of  $\frac{1}{N} \log Q_N \rightarrow \log \lambda_2$ . Hence we have the free energy  $F_{\text{conf}}$  as shown below:

$$\begin{aligned} F_{\text{conf}}(J_1, J_2, T) &= Nk_B T \{ \log [(1-x_1^2)(1-x_2^2)] - \log 2 \\ &\quad - \log [1 + x_2^2 - 2x_2x_1^2 \\ &\quad + (1-x_2) \sqrt{(1+x_2)^2 - 4x_2x_1^2}] \}, \end{aligned} \quad (12)$$

in the thermodynamic limit.

From this configurational free energy  $F_{\text{conf}}$  evaluated from the partition function, which is an analytical function for all  $J_1, J_2$  when  $T > 0\text{K}$ , one may draw the following inferences:

(1) The occurrence of phase transition at finite temperature is ruled out because the partition function of the system, which reads  $e^{-F_{\text{conf}}/k_B T}$ , encounters no singularities (as visualized in FIG. 2) in the thermodynamic limit when  $T > 0\text{K}$  because the argument of the logarithm never vanishes in such cases. In other words, the system has only one phase for any non-zero absolute temperature.

(2) The configurational entropy  $S_{\text{conf}}$  could be evaluated by

$$\begin{aligned} \frac{S_{\text{conf}}}{Nk_B} &= -\frac{1}{Nk_B} \frac{\partial F_{\text{conf}}}{\partial T} \\ &= -\frac{1}{4x_2} \left\{ (1+x_2^2) \frac{J_2}{k_B T} + (1-x_2) \times \right. \\ &\quad \left. [-(1+x_2)^2 \frac{J_2}{k_B T} + 2x_2x_1 \frac{J_1}{k_B T}] \times \right. \\ &\quad \left. [(1+x_2)^2 - 4x_2x_1^2]^{-1/2} \right\} + \log 2 \\ &\quad - \log [(1-x_1^2)(1-x_2^2)] \\ &\quad + \log [1 + x_2^2 - 2x_2x_1^2 \\ &\quad + (1-x_2) \sqrt{(1+x_2)^2 - 4x_2x_1^2}]. \end{aligned} \quad (13)$$

where  $\hat{L} = \text{diag}[\lambda_1, \lambda_2, \lambda_3, \lambda_4]$  is a matrix with four eigenvalues of  $\hat{T}$  as its diagonal elements. Therefore,  $Q_N = \lambda_1^N + \lambda_2^N + \lambda_3^N + \lambda_4^N$ . Here,

(3) The short-range correlation functions  $\langle \sigma_k \sigma_{k+1} \rangle$  and  $\langle \sigma_k \sigma_{k+2} \rangle$  ( $\langle \cdot \rangle$ : ensemble average) read:

$$\begin{aligned} \langle \sigma_k \sigma_{k+1} \rangle &= \frac{4k_B T}{N} \frac{\partial}{\partial J_1} \left( \frac{1}{2} F_{\text{conf}} \right) \\ &= -\frac{(1-x_2)x_1}{\sqrt{(1+x_2)^2 - 4x_2x_1^2}} \end{aligned} \quad (14)$$

$$\begin{aligned} \langle \sigma_k \sigma_{k+2} \rangle &= \frac{4k_B T}{N} \frac{\partial}{\partial J_2} \left( \frac{1}{2} F_{\text{conf}} \right) \\ &= -\frac{1+x_2^2 - \frac{(1-x_2^2)(1+x_2)}{\sqrt{(1+x_2)^2 - 4x_2x_1^2}}}{2x_2} \end{aligned} \quad (15)$$

(4)  $S_{\text{conf}}, \langle \sigma_k \sigma_{k+1} \rangle$  and  $\langle \sigma_k \sigma_{k+2} \rangle$  changes continuously as the temperature approaches absolute zero.

The equation

$$S_{\text{conf}}(J_1, J_2, T) \rightarrow 0, \text{ as } T \rightarrow 0\text{K}, \quad (16)$$

is in accordance with the third law of thermodynamics; the equations<sup>29</sup>

$$\langle \sigma_k \sigma_{k+1} \rangle \rightarrow -1, \text{ as } T \rightarrow 0\text{K}; \quad (17)$$

$$\langle \sigma_k \sigma_{k+2} \rangle \rightarrow +1, \text{ as } T \rightarrow 0\text{K}. \quad (18)$$

agree with the intuitive picture at absolute zero: NN sites should contain one atom fixed at one site and one vacancy at the other (hence  $\langle n_k n_{k+1} \rangle = 0$ ,  $\langle \sigma_k \sigma_{k+1} \rangle = -1$  for all  $k$ ); NNN sites should be both occupied or both vacant (hence  $\langle n_{2k} n_{2k+2} \rangle = 0$ ,  $\langle n_{2k-1} n_{2k+1} \rangle = 1$ ,  $\langle \sigma_k \sigma_{k+2} \rangle = +1$  for all  $k$ ).

## B. Ensemble Expectation and Correlations via the Transfer Matrix

Now we will employ the transfer matrix<sup>27,28</sup> to prove that the ensemble expectation  $\langle \Sigma_k \rangle$  vanishes in the ther-

modynamic limit for all  $k$  at finite temperature, which infers the vanishment of the right side of Eqn. (6). This will not only justify our procedure of lifting the ‘‘atom-number conservation’’ constraint but also show that the long-range order is non-existent at finite temperature.

We find that

$$\begin{aligned}
\langle \Sigma_k \rangle &= \frac{1}{Q_N} \sum_{(\sigma)} \Sigma_k \times \\
&\exp \left[ -\beta' \sum_{k=1}^{2N} (J_1 \sigma_k \sigma_{k+1} + J_2 \sigma_k \sigma_{k+2}) \right] \\
&= \frac{1}{Q_N} \sum_{(\sigma)} \hat{T}_{\Sigma_1 \Sigma_2} \hat{T}_{\Sigma_2 \Sigma_3} \cdots \\
&\cdots \left( \hat{T}_{\Sigma_{k-1} \Sigma_k} \Sigma_k \hat{T}_{\Sigma_k \Sigma_{k+1}} \right) \cdots \hat{T}_{\Sigma_{N-1} \Sigma_N} \\
&= \frac{1}{Q_N} \sum_{(\sigma)} \hat{T}_{\Sigma_1 \Sigma_2} \hat{T}_{\Sigma_2 \Sigma_3} \cdots \\
&\cdots \left( \hat{A}_{\Sigma_{k-1} \Sigma_{k+1}} \right) \cdots \hat{T}_{\Sigma_{N-1} \Sigma_N}. \tag{19}
\end{aligned}$$

Here,  $\hat{A} = \hat{T} (\hat{\sigma}_z \otimes \hat{1} + i \hat{1} \otimes \hat{\sigma}_z) \hat{T}$ ,  $\hat{\sigma}_z$  is the Pauli matrix and

$$\begin{aligned}
&\hat{\sigma}_z \otimes \hat{1} + i \hat{1} \otimes \hat{\sigma}_z \\
&= \begin{bmatrix} 1+i & 0 & 0 & 0 \\ 0 & 1-i & 0 & 0 \\ 0 & 0 & -1+i & 0 \\ 0 & 0 & 0 & -1-i \end{bmatrix}. \tag{20}
\end{aligned}$$

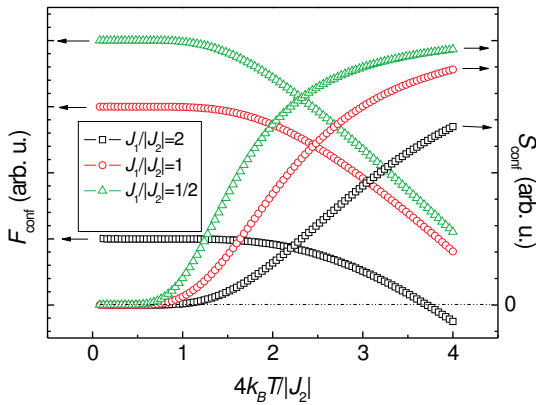


FIG. 2: This plots configurational free energy  $F_{\text{conf}}$  and entropy  $S_{\text{conf}}$  versus temperature for various  $J_1/J_2$  ratios.  $S_{\text{conf}}=0$  at 0K in all these cases.

Therefore,

$$\begin{aligned}
\langle \Sigma_k \rangle &= \frac{1}{Q_N} \text{Tr} \left[ \left( \hat{\sigma}_z \otimes \hat{1} + i \hat{1} \otimes \hat{\sigma}_z \right) \hat{T}^N \right] \\
&= \frac{1}{Q_N} \text{Tr} \left[ \hat{S}^{-1} \left( \hat{\sigma}_z \otimes \hat{1} + i \hat{1} \otimes \hat{\sigma}_z \right) \hat{S} \hat{L}^N \right]. \tag{21}
\end{aligned}$$

As a matter of fact,  $\hat{S}^{-1} (\hat{\sigma}_z \otimes \hat{1} + i \hat{1} \otimes \hat{\sigma}_z) \hat{S}$  takes the shape of

$$\begin{bmatrix} 0 & 0 & a & b \\ 0 & 0 & c & d \\ e & f & 0 & 0 \\ g & h & 0 & 0 \end{bmatrix} \tag{22}$$

where the eight Latin letters represent the elements that

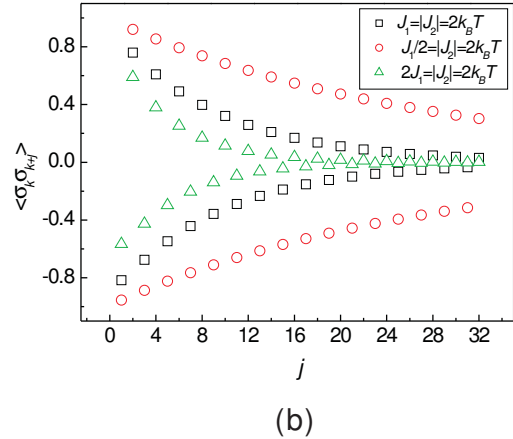
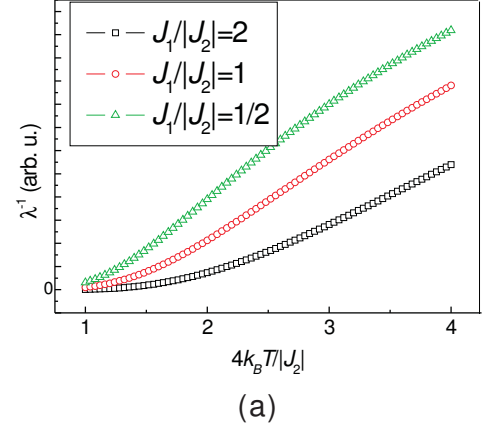


FIG. 3: (a) The inverse correlation length  $\lambda^{-1}$  versus temperature for various  $J_1/J_2$  ratios. Note that as  $T$  approaches absolute zero, so does  $\lambda^{-1}$  because the correlation length is  $\infty$  at 0K. (b) The correlation function  $\langle \sigma_k \sigma_{k+j} \rangle$  versus  $j$  for fixed temperature and  $J_1/J_2$  ratios.

are not necessarily zero.

$$\begin{aligned} & \text{Tr} \left[ \widehat{S}^{-1} \left( \widehat{\sigma}_z \otimes \widehat{1} + i\widehat{1} \otimes \widehat{\sigma}_z \right) \widehat{S} \widehat{L}^N \right] \\ = & \text{Tr} \begin{bmatrix} 0 & 0 & a\lambda_3^N & b\lambda_4^N \\ 0 & 0 & c\lambda_3^N & d\lambda_4^N \\ e\lambda_1^N & f\lambda_2^N & 0 & 0 \\ g\lambda_1^N & h\lambda_2^N & 0 & 0 \end{bmatrix} = 0. \end{aligned} \quad (23)$$

It is now evident that in the limit that  $N \rightarrow \infty$ ,  $\langle \Sigma_k \rangle \rightarrow 0$ , which is equivalent to

$$\sum_{j=1}^N \sigma_{2j} = \sum_{j=1}^N \sigma_{2j-1} = 0, \quad (24)$$

which is an indication of vanishing long-range order at finite temperature because Eqn. (24) suggests that the interstitial sites are occupied by  $N/2$  atoms and so are the lattice sites.

From this result, we may conclude that unlike the short-range parameters such as  $\langle \sigma_k \sigma_{k+1} \rangle$  and  $\langle \sigma_k \sigma_{k+2} \rangle$ , the long-range order parameter  $\mathfrak{L}$  witnesses a catastrophe at 0K:

$$L \equiv \frac{1}{2N} \sum_{k=1}^{2N} (-1)^k \langle 2n_k - 1 \rangle = \begin{cases} \pm 1, & T = 0\text{K} \\ 0, & T > 0\text{K} \end{cases} \quad (25)$$

Therefore, there exists a solid-liquid phase transition at 0K, a process characterized by destruction of long-range order and preservation of short-range order in the meantime.

To obtain the correlation between  $\Sigma_k$  at different sites, we may extend the matrix method to the correlation function  $\Gamma(k, k+j)$  (for simplicity,  $j$  is assumed to be positive hereinafter):

$$\begin{aligned} & \Gamma(k, k+j) \\ \equiv & \langle (\Sigma_k - \langle \Sigma_k \rangle) (\Sigma_{k+j} - \langle \Sigma_{k+j} \rangle) \rangle = \langle \Sigma_k \Sigma_{k+j} \rangle \\ = & \frac{1}{Q_N} \text{Tr} \left[ \widehat{S}^{-1} \left( \widehat{\sigma}_z \otimes \widehat{1} + i\widehat{1} \otimes \widehat{\sigma}_z \right) \widehat{S} \widehat{L}^j \widehat{S}^{-1} \left( \widehat{\sigma}_z \otimes \widehat{1} + i\widehat{1} \otimes \widehat{\sigma}_z \right) \widehat{S} \widehat{L}^{N-j} \right] \\ = & \frac{1}{Q_N} \times \\ & \text{Tr} \left\{ \begin{bmatrix} \left[ \begin{matrix} ae \left( \frac{\lambda_3}{\lambda_1} \right)^j + bg \left( \frac{\lambda_4}{\lambda_1} \right)^j \\ ce \left( \frac{\lambda_3}{\lambda_1} \right)^j + dg \left( \frac{\lambda_4}{\lambda_1} \right)^j \end{matrix} \right] \lambda_1^N & \left[ \begin{matrix} af \left( \frac{\lambda_3}{\lambda_2} \right)^j + bh \left( \frac{\lambda_4}{\lambda_2} \right)^j \\ cf \left( \frac{\lambda_3}{\lambda_2} \right)^j + dh \left( \frac{\lambda_4}{\lambda_2} \right)^j \end{matrix} \right] \lambda_2^N \\ \oplus & \left[ \begin{matrix} ae \left( \frac{\lambda_1}{\lambda_3} \right)^j + cf \left( \frac{\lambda_2}{\lambda_3} \right)^j \\ ag \left( \frac{\lambda_1}{\lambda_3} \right)^j + ch \left( \frac{\lambda_2}{\lambda_3} \right)^j \end{matrix} \right] \lambda_3^N & \left[ \begin{matrix} be \left( \frac{\lambda_1}{\lambda_4} \right)^j + df \left( \frac{\lambda_2}{\lambda_4} \right)^j \\ bg \left( \frac{\lambda_1}{\lambda_4} \right)^j + dh \left( \frac{\lambda_2}{\lambda_4} \right)^j \end{matrix} \right] \lambda_4^N \end{bmatrix} \right\} \\ \rightarrow & cf \left( \frac{\lambda_3}{\lambda_2} \right)^j + dh \left( \frac{\lambda_4}{\lambda_2} \right)^j = cfe^{-\frac{2j}{\mu}} + dhe^{-\frac{2j}{\lambda}}. \end{aligned} \quad (26)$$

where

$$\frac{cf}{i} = \frac{(1-x_2) \left[ \sqrt{(1+x_2)^2 - 4x_2x_1^2} - x_1 \sqrt{(1+x_2)^2 x_1^2 - 4x_2} \right]}{\sqrt{(1+x_2)^2 x_1^2 - 4x_2} \sqrt{(1+x_2)^2 - 4x_2x_1^2}}, \quad (27)$$

$$\frac{dh}{i} = - \frac{(1-x_2) \left[ \sqrt{(1+x_2)^2 - 4x_2x_1^2} + x_1 \sqrt{(1+x_2)^2 x_1^2 - 4x_2} \right]}{\sqrt{(1+x_2)^2 x_1^2 - 4x_2} \sqrt{(1+x_2)^2 - 4x_2x_1^2}}, \quad (28)$$

and  $\mu \ll \lambda$ ,

$$\mu = 2 \left( \log \frac{\lambda_2}{\lambda_3} \right)^{-1} = 2 \left[ \log \frac{1 + x_2^2 - 2x_2x_1^2 + (1 - x_2) \sqrt{(1 + x_2)^2 - 4x_2x_1^2}}{x_1^2 - (1 - x_2)x_1 \sqrt{(1 + x_2)^2 - 4x_2x_1^2}} \right]^{-1}, \quad (29)$$

$$\lambda = 2 \left( \log \frac{\lambda_2}{\lambda_4} \right)^{-1} = 2 \left[ \log \frac{1 + x_2^2 - 2x_2x_1^2 + (1 - x_2) \sqrt{(1 + x_2)^2 - 4x_2x_1^2}}{x_1^2 + (1 - x_2)x_1 \sqrt{(1 + x_2)^2 - 4x_2x_1^2}} \right]^{-1}. \quad (30)$$

With the definition of  $\Sigma_k$ , we obtain that

$$\begin{aligned} \langle \Sigma_k \Sigma_{k+j} \rangle &= (\langle \sigma_{2k-1} \sigma_{2k+2j-1} \rangle - \langle \sigma_{2k} \sigma_{2k+2j} \rangle) \\ &\quad + i (\langle \sigma_{2k-1} \sigma_{2k+2j} \rangle + \langle \sigma_{2k} \sigma_{2k+2j-1} \rangle) \end{aligned} \quad (31)$$

Therefore,  $\langle \sigma_{2k-1} \sigma_{2k+2j-1} \rangle - \langle \sigma_{2k} \sigma_{2k+2j} \rangle = 0$  (translational invariance) and

$$\begin{aligned} &G(0, 2j+1) + G(0, 2j-1) \\ &= \langle \sigma_{2k-1} \sigma_{2k+2j} \rangle + \langle \sigma_{2k} \sigma_{2k+2j-1} \rangle \\ &= \frac{cf}{i} \left( \frac{\lambda_3}{\lambda_2} \right)^j + \frac{dh}{i} \left( \frac{\lambda_4}{\lambda_2} \right)^j. \end{aligned} \quad (32)$$

Similarly, we explore the properties of  $\Sigma'_k = \sigma_{2k-1} - \sigma_{2k}$  (obtained by replacing the factor  $i$  in  $\Sigma_k$  with  $-1$ ) by the following procedures:

(1)  $\widehat{S}^{-1}(\widehat{\sigma}_z \otimes \widehat{1} - \widehat{1} \otimes \widehat{\sigma}_z)\widehat{S}$  takes the shape of

$$\begin{bmatrix} 0 & 0 & \alpha & \beta \\ 0 & 0 & \chi & \delta \\ \varepsilon & \phi & 0 & 0 \\ \gamma & \eta & 0 & 0 \end{bmatrix}; \quad (33)$$

where each Greek letter represents a non-vanishing element.

(2) Verify that

$$\begin{aligned} &\langle \Sigma'_k \Sigma'_{k+j} \rangle \\ &= (\langle \sigma_{2k-1} \sigma_{2k+2j-1} \rangle + \langle \sigma_{2k} \sigma_{2k+2j} \rangle) - (\langle \sigma_{2k-1} \sigma_{2k+2j} \rangle + \langle \sigma_{2k} \sigma_{2k+2j-1} \rangle) \\ &= 2G(0, 2j) - [G(0, 2j+1) + G(0, 2j-1)] \\ &= \frac{1}{Q_N} \text{Tr} \left[ \widehat{S}^{-1} (\widehat{\sigma}_z \otimes \widehat{1} - \widehat{1} \otimes \widehat{\sigma}_z) \widehat{S} \widehat{L}^j \widehat{S}^{-1} (\widehat{\sigma}_z \otimes \widehat{1} - \widehat{1} \otimes \widehat{\sigma}_z) \widehat{S} \widehat{L}^{N-j} \right] \\ &\rightarrow \chi \phi \left( \frac{\lambda_3}{\lambda_2} \right)^j + \delta \eta \left( \frac{\lambda_4}{\lambda_2} \right)^j. \end{aligned} \quad (34)$$

Then we combine the results above to find the recursion relations:

$$G(0, 2j) = \frac{1}{2} \left[ \left( \frac{cf}{i} + \chi \phi \right) \left( \frac{\lambda_3}{\lambda_2} \right)^j + \left( \frac{dh}{i} + \delta \eta \right) \left( \frac{\lambda_4}{\lambda_2} \right)^j \right]; \quad (35)$$

$$G(0, 2j+1) + G(0, 2j-1) = \frac{cf}{i} \left( \frac{\lambda_3}{\lambda_2} \right)^j + \frac{dh}{i} \left( \frac{\lambda_4}{\lambda_2} \right)^j, \quad (36)$$

and the initial condition

$$G(0, 1) = \langle \sigma_k \sigma_{k+1} \rangle = - \frac{(1 - x_2) x_1}{\sqrt{(1 + x_2)^2 - 4x_2x_1^2}} \quad (37)$$

which finally results in

$$\begin{aligned}
G(0, j) &= \langle \sigma_k \sigma_{k+j} \rangle \\
&= \frac{1}{2} \left(1 - (-1)^j\right) \left[ \frac{cf}{i \left(\frac{\lambda_3}{\lambda_2} + 1\right)} \left(\frac{\lambda_3}{\lambda_2}\right)^{\frac{j+1}{2}} + \frac{dh}{i \left(\frac{\lambda_4}{\lambda_2} + 1\right)} \left(\frac{\lambda_4}{\lambda_2}\right)^{\frac{j+1}{2}} \right] \\
&\quad + \frac{1}{4} \left(1 + (-1)^j\right) \left[ \left(\frac{cf}{i} + \chi\phi\right) \left(\frac{\lambda_3}{\lambda_2}\right)^{\frac{j}{2}} + \left(\frac{dh}{i} + \delta\eta\right) \left(\frac{\lambda_4}{\lambda_2}\right)^{\frac{j}{2}} \right] \\
&= \frac{1}{2} \left(1 - (-1)^j\right) \left(Ae^{-\frac{|j|+1}{\mu}} + Be^{-\frac{|j|+1}{\lambda}}\right) + \frac{1}{4} \left(1 - (-1)^j\right) \left(A'e^{-\frac{|j|}{\mu}} + B'e^{-\frac{|j|}{\lambda}}\right). \tag{38}
\end{aligned}$$

where

$$A = \frac{cf}{i \left(\frac{\lambda_3}{\lambda_2} + 1\right)} = \frac{(1+x_2)^2(1-x_1^2) - (1-x_2) \left[ x_1 \sqrt{(1+x_2)^2 x_1^2 - 4x_2} - \sqrt{(1+x_2)^2 - 4x_2 x_1^2} \right]}{2\sqrt{(1+x_2)^2 x_1^2 - 4x_2} \sqrt{(1+x_2)^2 - 4x_2 x_1^2}}; \tag{39}$$

$$B = \frac{dh}{i \left(\frac{\lambda_4}{\lambda_2} + 1\right)} = \frac{-(1+x_2)^2(1-x_1^2) - (1-x_2) \left[ x_1 \sqrt{(1+x_2)^2 x_1^2 - 4x_2} + \sqrt{(1+x_2)^2 - 4x_2 x_1^2} \right]}{2\sqrt{(1+x_2)^2 x_1^2 - 4x_2} \sqrt{(1+x_2)^2 - 4x_2 x_1^2}}; \tag{40}$$

$$A' = \frac{cf}{i} + \chi\phi = 1 - \frac{(1-x_2)^2 x_1}{\sqrt{(1+x_2)^2 x_1^2 - 4x_2} \sqrt{(1+x_2)^2 - 4x_2 x_1^2}}; \tag{41}$$

$$B' = \frac{dh}{i} + \delta\eta = 1 + \frac{(1-x_2)^2 x_1}{\sqrt{(1+x_2)^2 x_1^2 - 4x_2} \sqrt{(1+x_2)^2 - 4x_2 x_1^2}}. \tag{42}$$

For large  $|j|$ , the  $e^{-|j|/\lambda}$  terms dominate the correlation function  $\langle \sigma_k \sigma_{k+j} \rangle$ , so  $\lambda$  serves as the correlation length that characterizes the maximum range of information transfer in the 1D atom chain. (This is visualized in FIG. 3)

### C. Discussions

From the exact solutions of  $F_{\text{conf}}$  and  $\langle \Sigma_k \rangle$ , we find that the 1D atom chain “melts” at 0K. The catastrophe of long-range order and continuous change of short-range order compare reasonably with a real solid-liquid phase transition in three dimensions. This melting point in 1D atom chain is in perfect agreement with the Lindemann criterion in the 1D case, recalling the well-established result that the mean displacement of a 1D elastic atom chain is  $\infty$  for any positive temperature<sup>32</sup>. Although in the model Hamiltonian Eqn. (1), we do not explicitly take vibrational energy into account, the melting point in our

model still coincides with the prediction based on vibrational instability for two reasons: (1) the pair interaction mode in our model (a repulsion  $J_1$  for NN, an attraction  $J_2$  for NNN, say) still forms a reasonable caricature of the potential well in a solid. (2) the “hopping” between lattice sites and interstitialcy sites, which is the mode of atom movement in our model, mimics the quantized motion of atoms at low temperature.

One may also check Born’s scenario in our 1D exact solution. In principle, there is no such a counterpart of the three-dimensional shear moduli in the 1D case. Nevertheless, for fixed  $J_2$  (bonding energy), greater  $J_1$  infers greater energy gap between the NN contact and NNN contact modes. In other words, when the bonding energy  $J_2$  and temperature  $T$  is fixed, increasing  $J_1$  will add to the difficulty of creating interstitialcies, thereby increasing the “rigidity” of the 1D atom chain. In the light of this, we may define a dimensionless “rigidity parameter” as  $(J_1 + |J_2|) / |J_2|$ . It can be verified analytically that

$$\begin{aligned}
& \left( \frac{\partial S_{\text{conf}}(J_1, J_2, T)}{\partial J_1} \right)_{J_2, T} = \frac{(1-x_1^2)}{4k_B T} \left( \frac{\partial S_{\text{conf}}(x_1, x_2)}{\partial x_1} \right)_{x_2} \\
& = \frac{(1-x_1^2)}{4k_B T} \frac{2(x_2-1)(x_2+1)^2}{\sqrt{[(1+x_2)^2 - 4x_1^2 x_2]^3}} (\tanh^{-1} x_1 - 2x_1 \tanh^{-1} x_2) \\
& < 0, (0 < -x_2, x_1 < 1)
\end{aligned} \tag{43}$$

and

$$\begin{aligned}
& \left( \frac{\partial \lambda(J_1, J_2, T)}{\partial J_1} \right)_{J_2, T} = \frac{(1-x_1^2)}{4k_B T} \left( \frac{\partial \lambda(x_1, x_2)}{\partial J_1} \right)_{x_2} \\
& = \lambda^2 \frac{2(1-x_2)}{4k_B T} \left[ \frac{1}{\sqrt{x_1^2(1+x_2)^2 - 4x_2}} - \frac{1}{\sqrt{\frac{1}{x_1^2}(1+x_2)^2 - 4x_2}} \right] \\
& > 0, (0 < -x_2, x_1 < 1)
\end{aligned} \tag{44}$$

Physically speaking, these two inequalities are reasonable because the increase of rigidity will help to restore some short range order to the system, thereby lowering the entropy and increasing the correlation length. (See FIG. 2 and FIG. 3(a) for specific examples.)

The exact solution above provides insight for the 3D case in that correlation between atom occupancies stands to be the common means to propagate instability in systems, no matter what dimensionality. In a proceeding paper, we will present a detailed analysis of how such correlation undermines the long-range order in a fcc crystal. Some numerical corollaries of this 1D model may also shed light on the melting point formula to be established in the 3D case.<sup>30</sup> One heuristic approach to “guess” the melting point formula in 3D is to find the “critical” temperature  $T_c$  in the 1D model where the heat capacity has a maximum, and speculate that such a  $T_c$  will correspond to a heat capacity discontinuity in the 3D case. A lengthy expression for the heat capacity

$$c = T \frac{\partial S_{\text{conf}}}{\partial T} \tag{45}$$

in our 1D model could be obtained analytically. FIG. 4 presents a “phase diagram” for the sign of  $\partial c/\partial T$  based on the analytical expression, in which the phase boundary (where  $\partial c/\partial T = 0$ ) could be approximated by a simple formula<sup>31</sup>:

$$\tanh \frac{|J_1|}{4k_B T_c} + \tanh \frac{|J_2|}{4k_B T_c} \approx 0.88. \tag{46}$$

When  $|J_1| \approx |J_2|$ , the formula above could be replaced by

$$|J_1| + |J_2| \approx 3.52k_B T_c \tag{47}$$

without loss of precision. This suggests that in the scenario of 3D melting at a temperature corresponding to

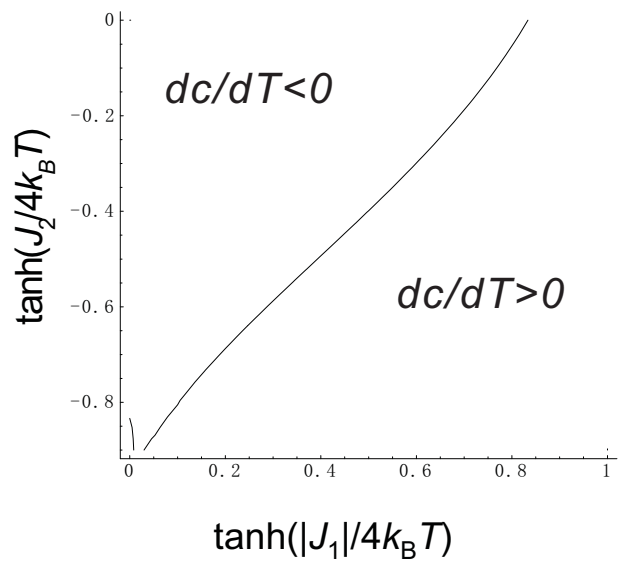


FIG. 4: A “phase diagram” for  $\partial c/\partial T$  ( $c$ : heat capacity;  $T$ : absolute temperature) in which the phase boundary is approximately a straight line.

such a  $T_c$ , the thermal energy  $\sim 3k_B T_c$  is roughly tantamount to the energy barrier of interstitialcy creation, or in other words, the “rigidity” is combatted by thermal motion. As long as such a positive  $T_c$  is existent, we hold the following to be true:

$$\tanh \frac{|J_2|}{4k_B T_c} \lesssim 0.88, T_c \gtrsim \frac{|J_2|}{5.5k_B}. \tag{48}$$



#### IV. SUMMARY

We find an exact solution to the 1D problem, in which the atom chain “melts” at 0K, which is consistent with the Lindemann criterion in the 1D case. The behavior of the atom chain also suggests that softer lattice has greater disorder, because for fixed temperature  $T$  and “bonding energy”  $|J_2|$ , both the configurational entropy (FIG. 3(a)) and the inverse correlation length (FIG. 3(b)) increase monotonically with the decreasing of the dimensionless “rigidity parameter”  $(J_1 + |J_2|) / |J_2|$  – manifesting the reasonability of Born’s criterion.

#### Acknowledgments

This work is supported by National Natural Science Foundation of China and 973 project.

### APPENDIX A: AN GRAPH THEORETIC APPROACH IN 1D ATOM CHAIN

#### 1. An Exact Graph Theoretic Approach for 1D Chain Composed of Finite Atoms

The main idea of our graph theoretic solution is parallel to that of Kac, Ward<sup>33</sup>, and Vdovichenko<sup>34</sup>, as referred to in some textbooks. (e.g. See Ref.<sup>27,35</sup>) However, the Feynman rules involved in our calculation are non-trivial and should be carefully developed. Furthermore, the evaluation of the thermodynamic limit requires considerable techniques. For the completeness of this Appendix, we will elaborate on the solution process in three steps.

(1) We use the identity

$$\exp(\tau\theta) = \cosh\theta(1 + \tau \tanh\theta), \tau = \pm 1 \quad (\text{A1})$$

and substitutions  $x_1 = \tanh(J_1/4k_B T)$ ,  $x_2 = \tanh(J_2/4k_B T)$  to transform the partition function into

$$Q_N = (1 - x_1^2)^{-N} (1 - x_2^2)^{-N} S(x_1, x_2) \quad (\text{A2})$$

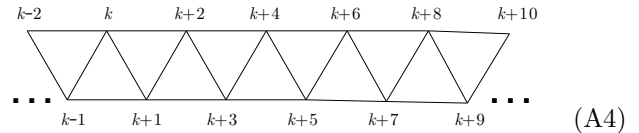
where

$$S(x_1, x_2) = \sum_{\{\sigma_k = \pm 1\}} \prod_{k=1}^{2N} (1 - x_1 \sigma_k \sigma_{k+1}) (1 - x_2 \sigma_k \sigma_{k+2}) \quad (\text{A3})$$

The summand in Eqn. (A3) is a polynomial in the variables  $x_1, x_2$  and  $\sigma_k$ . Each  $\sigma_k$  can appear in the polynomial in powers ranging from zero to four. After summation over all the  $\{\sigma_k = \pm 1\}$  states, the terms containing odd powers of  $\sigma_k$  would vanish. Therefore, a non-zero contribution comes only from terms containing  $\sigma_k$  in powers of 0, 2 or 4. Since  $\sigma_k^0 = \sigma_k^2 = \sigma_k^4 = 1$ , each

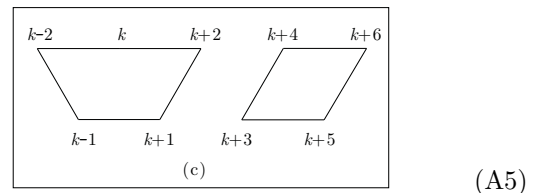
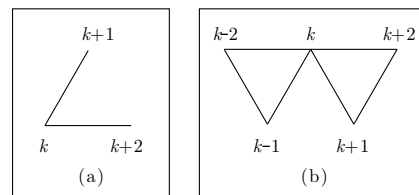
term of the polynomial which contains all the variables  $\sigma_k$  in even powers gives a contribution to the sum which is proportional to the number of configurations,  $2^{2N}$ .

(2) We notice that each term of the polynomial can be uniquely related to a set of lines or “bonds” joining various pairs of adjoining lattice points as shown in FIG. (A4).



For instance, the diagrams in FIG. (A5) correspond to the terms

- (a)  $x_1 x_2 \sigma_{k+1} \sigma_k^2 \sigma_{k+2}$ ,
- (b)  $x_1^4 x_2^2 \sigma_{k-2}^2 \sigma_{k-1}^2 \sigma_k^4 \sigma_{k+1}^2 \sigma_{k+2}^2$ ,
- (c)  $-x_1^4 x_2^5 \sigma_{k-2}^2 \sigma_{k-1}^2 \sigma_{k+1}^2 \sigma_{k+2}^2 \sigma_k^2 \sigma_{k+4}^2 \sigma_{k+3}^2 \sigma_{k+5}^2 \sigma_{k+6}^2$ .



Each level line (alias “edge”) in the diagram is assigned a factor  $(-x_2)$  while each oblique line a factor  $(-x_1)$ . Each end of each line is associated with a factor  $\sigma_k$ . The fact that a non-zero contribution to the partition function comes only from terms in the polynomial which contain all the  $\sigma_k$  in even powers signifies geometrically that either 2 or 4 bonds must end at each point in the diagram.<sup>36</sup> Hence the summation is taken only over closed diagrams, which may be self-intersecting (as at the point numbered  $k$  in FIG. (A5) (b)).

In the light of this, the sum  $S(x_1, x_2)$  may be expressed in the form

$$S(x_1, x_2) = 2^{2N} \sum_r (-x_2)^r g_r \left( \frac{x_1}{x_2} \right) \quad (\text{A6})$$

where  $g_r$  is a polynomial with argument  $x_1/x_2$ . This polynomial represents the contributions from closed diagrams formed from a number  $r$  of bonds, with the coefficient of  $(x_1/x_2)^q$  being equal to the number of distinct  $r$ -bond long closed diagrams with an (even) number  $q$  of

oblique lines, and each multiple diagram (e.g. FIG. (A5) (c)) being counted once.

(3) We convert the summation over closed diagrams

*Theorem:*

$$\begin{aligned} & \frac{S(x_1, x_2)}{2^{2N}} \\ &= \frac{1}{2^{2N}} \sum_{n=0}^{2^{2N}-1} \left\{ \prod_{k=0}^{2N-1} \left[ 1 - x_2 (-1)^{\left( \lfloor \frac{n}{2^k \bmod 2N} \rfloor + \lfloor \frac{n}{2^{(k+2)} \bmod 2N} \rfloor \right)} \right] \left[ 1 - x_1 (-1)^{\left( \lfloor \frac{n}{2^k \bmod 2N} \rfloor + \lfloor \frac{n}{2^{(k+1)} \bmod 2N} \rfloor \right)} \right] \right\} \\ &= \left\{ \prod_{p=1}^{2N} \left[ \left( (1+x_2^2)(1-x_1^2) - 2x_2(1-x_1^2)f(p) \right)^2 + 2x_1^2(1-x_2)^4(1+f(p)) \right] \right\}^{1/4} \end{aligned} \quad (\text{A7})$$

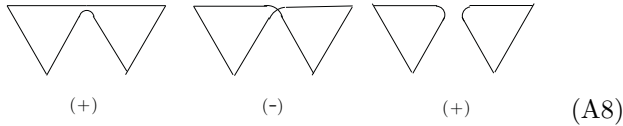
where

$$f(p) = \cos \frac{(2p+1 - (N \bmod 2))\pi}{N}$$

$\lfloor x \rfloor$  = the least integer that is greater than or equal to  $x$ .

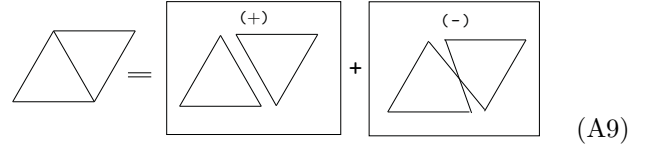
*Remark:* Every factor in the product above is non-negative in that it reaches the minimum value of  $(1+x_2)^4(1-x_1^2)^2 > 0$  at  $f(p) = -1$ .

We will regard each diagram as consisting of one or more closed loops. For non-self-intersecting diagrams this is obvious; for example, the diagram in FIG. (A5) (c) consists of two loops. For self-intersecting diagrams, however, the resolution into loops is not unique: a given diagram may consist of different numbers of loops for different ways of construction. This is illustrated by FIG. (A8), which shows three ways of representing the diagram in FIG. (A5) (b) as one or two non-self-intersecting loops or as one self-intersecting loop. (When referring to the number of intersections, we should be heedful that every turning point should be “polished” before being taken into computation.) Any intersection may similarly be traversed in three ways on more complicated diagrams.

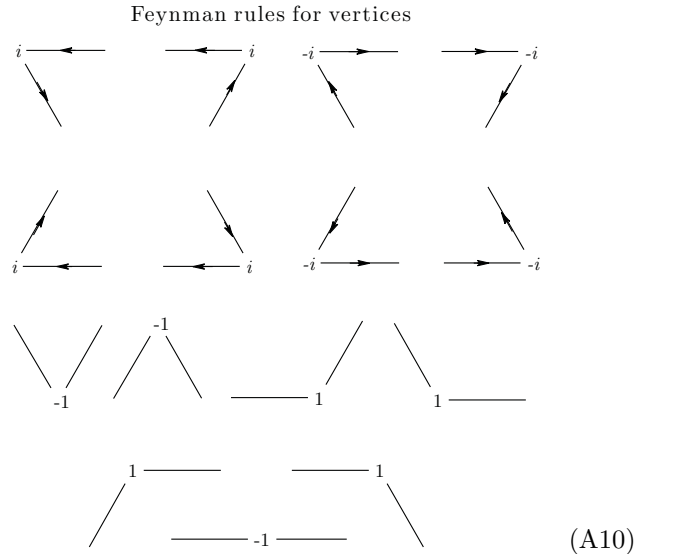


It is evident that the sum (A6) can be extended to all possible sets of loops if, in computing the contribution of diagrams to  $g_r(x_1/x_2)$ , each diagram is taken with the sign  $(-1)^n$ , where  $n$  is the total number of self-intersections in the loops of a given set, since when this is done all the extra terms in the sum necessarily cancel. For example, the three diagrams in FIG. (A8) have signs  $+$ ,  $-$ ,  $+$  respectively, so that two of them cancel, leaving a

single contribution to the sum, as they should. The new sum will also include diagrams with “repeated bonds”, of which the simplest example is shown in the far left of FIG. (A9):



These diagrams are not permissible, since some points have an odd number of bonds meeting at them, namely three, but in fact they cancel from the sum, as they should: when the loops corresponding to such a diagram are constructed each bond in common can be traversed in two ways, without intersection (as in the middle of FIG. (A9)) and with self-intersections (far right of FIG. (A9)); the resulting set of loops appear in the sum with opposite signs, and so cancel. We can also avoid the need to take into account explicitly the number of intersections by using the following Feynman rules:



Feynman rules for edges

$$\text{---} \underset{1}{\text{---}} \quad \diagup \underset{ix_1/x_2}{\text{---}} \quad \diagdown \underset{ix_1/x_2}{\text{---}} \quad . \quad (\text{A11})$$

It is a direct corollary from the rules above that every four-vertex contributes a factor 1 in general. It can be verified that when these rules are applied to diagrams in FIG. (A8), the product of all contributions from the edges and vertices results in the sign as  $(-1)^{s+n}$ , where  $n$  is the sum of number of self-intersections from a set of  $s$  loops.<sup>37</sup> Here is another more sophisticated example where contributions from the six oblique edges are not explicitly marked:

$$\begin{array}{c} -i \longrightarrow 1 \longleftarrow -1 \longleftarrow 1 \\ \diagdown \quad \diagup \quad \diagdown \quad \diagup \\ -1 \quad 1 \longrightarrow -1 \longrightarrow 1 \longrightarrow -i \end{array} = x_1^6/x_2^6 \quad . \quad (\text{A12})$$

It could be verified that the contribution of a directed graph does not change if all the arrows are reversed. Another thing that should be considered is that loops that “wrap up the circle” should bear a correct sign. When  $N$  is odd, this is automatically sufficed when the Feynman rules above are applied. For instance, the loop that connects all the consecutive sites together (and connects “ $2N$ ” to “1”) in a circle has the sign “-”. However, when  $N$  is even, we cannot achieve a correct counting unless we impose the following additional Feynman rules to the directed edges:

Additional Feynman rules for edges when  $N$  is even

$$\text{---} \underset{e^{-2i\epsilon}}{\text{---}} \quad \text{---} \underset{e^{2i\epsilon}}{\text{---}} \quad \diagup \underset{e^{i\epsilon}}{\text{---}} \quad \diagdown \underset{e^{i\epsilon}}{\text{---}} \quad \diagup \underset{e^{-i\epsilon}}{\text{---}} \quad \diagdown \underset{e^{-i\epsilon}}{\text{---}} \quad . \quad (\text{A13})$$

where  $\epsilon = \pi/2N$ .

We use these *ad hoc* Feynman rules instead of the “geometric result about the total angle of rotation of the tangent vector” (a variant of Umlaufsatz in differential geometry) as did in Ref. (35), because the latter method would result in different recurrence relations (see the argument below) for odd number sites and even number sites, which would plague the diagonalization procedure.

Let  $f_r(x_1/x_2)$  denote the sum over single loops of length  $r$  (i.e. consisting of  $r$  bonds), each loop carrying a factor  $\pm 1$  as determined by the Feynman rules, and the power of  $x_1/x_2$  denoting the number of oblique edges in that loop. Then the sum over all pairs of loops with total number of bonds  $r$  is

$$\frac{1}{2!} \sum_{r_1+r_2=r} f_{r_1} \left( \frac{x_1}{x_2} \right) f_{r_2} \left( \frac{x_1}{x_2} \right); \quad (\text{A14})$$

the factor  $1/2!$  takes into account the fact that the same pair of loops is obtained when the suffixes  $r_1$  and  $r_2$  are

interchanged, and similarly for loops of three or more loops. Thus the sum becomes

$$\begin{aligned} & \frac{S(x_1, x_2)}{2^{2N}} \\ &= \sum_{s=0}^{\infty} (-1)^s \frac{1}{s!} \sum_{r_1, r_2, \dots=1}^{\infty} (-x_2)^{r_1+\dots+r_s} \times \\ & f_{r_1} \left( \frac{x_1}{x_2} \right) \cdots f_{r_s} \left( \frac{x_1}{x_2} \right). \end{aligned} \quad (\text{A15})$$

Since  $S(x_1, x_2)$  includes sets of loops with every total length  $r_1 + r_2 + \dots$ , the numbers  $r_1, r_2, \dots$  in the inner sum take independently all values from 1 to  $\infty$ . Hence

$$\begin{aligned} & \sum_{r_1, r_2, \dots=1}^{\infty} (-x_2)^{r_1+\dots+r_s} f_{r_1} \left( \frac{x_1}{x_2} \right) \cdots f_{r_s} \left( \frac{x_1}{x_2} \right) \\ &= \left( \sum_{r=1}^{\infty} (-x_2)^r f_r \left( \frac{x_1}{x_2} \right) \right)^s \end{aligned} \quad (\text{A16})$$

and  $S(x_1, x_2)$  becomes

$$\frac{S(x_1, x_2)}{2^{2N}} = \exp \left( - \sum_{r=1}^{\infty} (-x_2)^r f_r \left( \frac{x_1}{x_2} \right) \right) \quad (\text{A17})$$

It is now convenient to assign to each lattice point (marked by an asterisk in the figure below) the four possible directions from it and to number them by a quantity  $\nu = 1, 2, 3, 4$ , say, as follows:

$$\begin{array}{ccc} 4 \longleftarrow \cdot \longrightarrow 1 & & \begin{array}{c} 3 \quad 2 \\ \diagdown \quad \diagup \\ 4 \longleftarrow \cdot \longrightarrow 1 \end{array} \end{array} \quad (\text{A18})$$

We define an auxiliary quantity  $W_r(k, \nu)$  the sum over all possible paths of length  $r$  from some given point  $k_0, \nu_0$  to a point  $k, \nu$  (each bond and vertex having as usual the factor contributed by Feynman rules); the final step to the point  $k, \nu$  must not be from a site marked by the left-right mirror of  $\nu$ . (e.g.  $1 \leftrightarrow 4, 2 \leftrightarrow 3$ ) With this definition,  $W_r(k_0, \nu_0)$  is the sum over all loops leaving the point  $k_0$  in the direction  $\nu_0$  and returning to that point. It is evident that

$$f_r \left( \frac{x_1}{x_2} \right) = \frac{1}{2r} \sum_{k_0, \nu_0} W_r(k_0, \nu_0); \quad (\text{A19})$$

both sides contain the sum over all single loops, but  $\sum W_r$  contains each loop  $2r$  times, since it can be traversed in two opposite direction and can be assigned to each of  $r$  starting points on it.

From the definition of  $W_r(k, \nu)$  we have the recurrence relations (sometimes referred to as Chapman-Kolmogorov equations) when  $N$  is an even number:

$$\left. \begin{aligned} W_{r+1}(k, 1) &= -e^{2i\varepsilon} W_r(k-2, 1) + i\frac{x_1}{x_2} e^{i\varepsilon} W_r(k-1, 2) + \frac{x_1}{x_2} e^{-i\varepsilon} W_r(k+1, 3) + 0 \\ W_{r+1}(k, 2) &= e^{2i\varepsilon} W_r(k-2, 1) - i\frac{x_1}{x_2} e^{i\varepsilon} W_r(k-1, 2) + 0 + i e^{-2i\varepsilon} W_r(k+2, 4) \\ W_{r+1}(k, 3) &= -i e^{2i\varepsilon} W_r(k-2, 1) + 0 - i\frac{x_1}{x_2} e^{-i\varepsilon} W_r(k+1, 3) + e^{-2i\varepsilon} W_r(k+2, 4) \\ W_{r+1}(k, 4) &= 0 - \frac{x_1}{x_2} e^{i\varepsilon} W_r(k-1, 2) + i\frac{x_1}{x_2} e^{-i\varepsilon} W_r(k+1, 3) - e^{-2i\varepsilon} W_r(k+2, 4) \end{aligned} \right\} \quad (\text{A20})$$

The method of constructing these relations is evident: for example, the point  $k, 1$  can be reached by taking the last  $(r+1)$ th step from the directions marked by 1, 2, 3, but not from the right (direction 4); the coefficients of  $W_r$  arise from the Feynman-rule contributions of the last bond and vertex encountered. We can verify that these coefficients are the same for odd number  $k$  and even number  $k$ . Let  $\Lambda$  denote the matrix of the coefficients in Eqs. (A20) (with all  $k$ ), written in the form

$$W_{r+1}(k, \nu) = \sum_{k', \nu'} \Lambda(k\nu|k'\nu') W_r(k', \nu').$$

The method of constructing these equations enables us to associate with this matrix an intuitive picture of a point moving step by step through the lattice with a “transitional probability” per step from one point to another which is equal to the corresponding element of the matrix  $\Lambda$ . The point traverses only one bond per step. It is evident that the “probability” of traversing a length  $r$  will be given by the matrix  $\Lambda^r$ . In particular the diagonal elements of this matrix give the “probability” that the point will return to its original position after traversing a loop of length  $r$ , i.e. they are equal to  $W_r(k_0, \nu_0)$ . Hence

$$\begin{aligned} \text{Tr}\Lambda^r &= \sum_{k_0, \nu_0} W_r(k_0, \nu_0), \\ f_r\left(\frac{x_1}{x_2}\right) &= \frac{1}{2r} \text{Tr}\Lambda^r = \frac{1}{2r} \sum_i \lambda_i^r, \end{aligned}$$

where the  $\lambda_i$  are the eigenvalues of the matrix. Substituting this expression in Eqn. (A17) and interchanging the order of summation over  $i$  and  $r$ , we obtain

$$\begin{aligned} \frac{S(x_1, x_2)}{2^{2N}} &= \exp\left\{-\frac{1}{2} \sum_i \sum_{r=1}^{\infty} \frac{1}{r} (-x_2)^r \lambda_i^r\right\} \\ &= \exp\left\{\frac{1}{2} \sum_i \log(1 + x_2 \lambda_i)\right\} \\ &= \sqrt{\prod_i (1 + x_2 \lambda_i)} \end{aligned} \quad (\text{A21})$$

The matrix  $\Lambda$  is easily diagonalized with respect to the suffix  $k$  by using a invertible transformation:

$$W_r(p, \nu) = \sum_{p=1}^{2N} e^{2ipk\varepsilon} W_r(k, \nu) \quad (\text{A22})$$

where  $\varepsilon = \pi/2N$ . Taking “Fourier components” on both sides of Eqs. (A20), we find that each equation contains only  $W_r(p, \nu)$  with the same  $p$ , so that the matrix  $\Lambda$  is diagonal with respect to  $p$ . For a given  $p$ , its elements are

$$\Lambda(p\nu|p\nu') = \begin{bmatrix} -e^{(2+4p)i\varepsilon} & i\frac{x_1}{x_2} e^{(1+2p)i\varepsilon} & +\frac{x_1}{x_2} e^{-(1+2p)i\varepsilon} & 0 \\ e^{(2+4p)i\varepsilon} & -i\frac{x_1}{x_2} e^{(1+2p)i\varepsilon} & 0 & i e^{-(2+4p)i\varepsilon} \\ -i e^{(2+4p)i\varepsilon} & 0 & -i\frac{x_1}{x_2} e^{-(1+2p)i\varepsilon} & e^{-(2+4p)i\varepsilon} \\ 0 & -\frac{x_1}{x_2} e^{(1+2p)i\varepsilon} & i\frac{x_1}{x_2} e^{-(1+2p)i\varepsilon} & -e^{-(2+4p)i\varepsilon} \end{bmatrix} \quad (\text{A23})$$

For a given  $p$ , a simple calculation shows that

$$\begin{aligned} \prod_{\nu=1}^4 (1 + x_2 \lambda_\nu) &= \det(\delta_{\nu\nu'} + x_2 \Lambda_{\nu\nu'}) \\ &= (1 + x_2^2)(1 - x_1^2) - 2x_2(1 - x_1^2) \cos \frac{(2p+1)\pi}{N} - 2ix_1(1 - x_2)^2 \cos \frac{(2p+1)\pi}{2N} \end{aligned} \quad (\text{A24})$$

where  $\lambda_\nu$  is the eigenvalue of block  $\Lambda(p\nu|p\nu')$ . Hence,

$$\Lambda(p\nu|p'\nu') = \bigoplus_{p=1}^{2N} \Lambda(p\nu|p\nu')$$

infers that

$$\frac{S(x_1, x_2)}{2^{2N}} = \left\{ \prod_{p=1}^{2N} \left[ (1+x_2^2)(1-x_1^2) - 2x_2(1-x_1^2) \cos \frac{(2p+1)\pi}{N} - 2ix_1(1-x_2)^2 \cos \frac{(2p+1)\pi}{2N} \right] \right\}^{1/2}. \quad (\text{A25})$$

For the odd  $N$  case, simply replace  $2p+1$  with  $2p$  and this would yield the correct result. The product in Eqn. (A7) is actually obtained by noticing that  $f_r(-x_1/x_2) = f_r(+x_1/x_2)$ , and by multiplying the Eqn. (A25) by its complex conjugate.

## 2. The Partition Function in the Thermodynamic Limit

In the thermodynamic limit, when  $N$  tends to infinity, the summation involved in the logarithm of the partition function can be legitimately replaced by a corresponding

integral. It can be seen that both odd  $N$  and even  $N$  lead to the same limit in the following integral, as they should:

$$\begin{aligned} & \lim_{N \rightarrow \infty} \frac{1}{2N} \log Q_N \\ &= -\frac{1}{2} [\log(1-x_2^2) + \log(1-x_1^2)] + \log 2 + \frac{1}{8\pi} I(x_1, x_2) \end{aligned}$$

where

$$I(x_1, x_2) = \int_0^{2\pi} \log \left\{ ((1+x_2^2)(1-x_1^2) - 2x_2(1-x_1^2) \cos 2\phi)^2 + 2x_1^2(1-x_2)^4(1+\cos 2\phi) \right\} d\phi \quad (\text{A26})$$

The integral involved in the partition could be evaluated with some complex analysis techniques as follows:

*Lemma:* Assume that  $a > 0$ ,  $\log 1 = 0$  and that  $t, s$  are real numbers, we have

$$\begin{aligned} I_1(a, t, s) &= \int_0^{2\pi} \log [a(1+t^2+s^2+2t(1+s)\cos m\phi+2s\cos 2m\phi)] d\phi \\ &= 2\pi \log a \end{aligned}$$

where

$$m = 1, 2, \dots, \min_{|z| \leq 1} |1+tz+sz^2| > 0. \quad (\text{A27})$$

*Proof:*

$$\begin{aligned} I_1(a, t, s) - 2\pi \log a &= 2\text{Re} \oint_{|z|=1} \log(1+tz^m+sz^{2m}) \frac{dz}{iz} \\ &= 2\text{Re} \left( 2\pi i \text{res} \left( \frac{\log(1+tz^m+sz^{2m})}{iz}, 0 \right) \right) = 0 \end{aligned} \quad (\text{A28})$$

■ *Corollary:*

$$\int_0^{2\pi} \log(a(1+t^2+2t\cos m\phi)) d\phi = 2\pi \log a, a > 0, -1 < t < 1, m = 1, 2, \dots \quad (\text{A29})$$

■ With these two lemmas, we are able to set out to evaluate the integral:

$$\begin{aligned} I_2(x_1, x_2) &= \int_0^{2\pi} \log \left\{ ((1+x_2^2)(1-x_1^2) - 2x_2(1-x_1^2) \cos 2\phi)^2 + 2x_1^2(1-x_2)^4(1+\cos 2\phi) \right\} d\phi \\ &= \int_0^{2\pi} \log \{ (1+x_2^2)^2(1-x_1^2)^2 + 2x_1^2(1-x_2)^4 + 2x_2^2(1-x_1^2)^2 \\ &\quad + (-4x_2(1+x_2^2)(1-x_1^2)^2 + 2x_1^2(1-x_2)^4) \cos 2\phi + 2x_2^2(1-x_1^2)^2 \cos 4\phi \} d\phi \end{aligned} \quad (\text{A30})$$

and reach the conclusion that

*Theorem:*

$$I_2(x_1, x_2) = 2\pi \log \left\{ \frac{1}{2} + \frac{1}{2}x_2^4 + 2x_2^2x_1^2 + x_2^2x_1^4 - 2x_1^2x_2 - 2x_1^2x_2^3 \right. \\ \left. + \frac{1}{2}(1-x_2)(x_2^2 - 2x_1^2x_2 + 1) \sqrt{(1+x_2)^2 - 4x_1^2x_2} \right\} \\ 0 \leq -x_2 < 1, 0 \leq x_1 < 1 \quad (\text{A31})$$

*Proof:* With

$$A = (1+x_2^2)^2(1-x_1^2)^2 + 2x_1^2(1-x_2)^4 + 2x_2^2(1-x_1^2)^2 \\ B = -4x_2(1+x_2^2)(1-x_1^2)^2 + 2x_1^2(1-x_2)^4 \\ C = 2x_2^2(1-x_1^2)^2 \quad (\text{A32})$$

and

$$a(1+t^2+s^2) = A > 0 \quad (\text{A33})$$

$$2at(1+s) = B > 0 \quad (\text{A34})$$

$$2as = C > 0, \quad (\text{A35})$$

and further that

we obtain

$$a(1+s+t)^2 = A+B+C \quad (\text{A36})$$

$$a(1+s-t)^2 = A-B+C \quad (\text{A37})$$

$$\frac{s}{(1+s)t} = \frac{C}{B} \quad (\text{A38})$$

$$\frac{(1+s)^2}{s} = \frac{B}{C} \frac{\sqrt{A+B+C} + \sqrt{A-B+C}}{\sqrt{A+B+C} - \sqrt{A-B+C}} \quad (\text{A39})$$

$$a = \frac{C}{2s} \\ = -\frac{1}{4(\sqrt{A-B+C} - \sqrt{A+B+C})} \times \\ \left[ \sqrt{A-B+C}(B+2C) + \sqrt{A+B+C}(B-2C) + \sqrt{2} \sqrt{B^2(A-3C + \sqrt{A-B+C}\sqrt{A+B+C})} \right] \\ = \frac{1}{2} + \frac{1}{2}x_2^4 + 2x_2^2x_1^2 + x_2^2x_1^4 - 2x_2x_1^2 - 2x_2^3x_1^2 + \frac{1}{2}(1-x_2)(x_2^2 - 2x_2x_1^2 + 1) \sqrt{(1+x_2)^2 + 4x_1^2 - x_2} \\ > 0 \quad (\text{A40})$$

From this, it is evident that  $s(x_1, x_2) = C/2a(x_1, x_2)$  is continuous with respect to  $(x_1, x_2)$  and  $s(x_1, x_2) > 0$  for  $0 < -x_2 < 1$ .

We are able to affirm that  $I_2(x_1, x_2) = 2\pi \log a(x_1, x_2)$  ( $0 < -x_2 < 1, 0 < x_1 < 1$ ) if we can further that  $\min_{|z| \leq 1} |1 + t(x_1, x_2)z + s(x_1, x_2)z^2| > 0$  is true for all  $(x_1, x_2)$  such that  $0 < -x_2 < 1, 0 < x_1 < 1$ . To verify this, we notice that for  $0 < -x_2 < 1, a(0, x_2) = 1, t(0, x_2) = -2x_2, s(0, x_2) = 2x_2^2$ , so it is easy to find

that  $\min_{|z| \leq 1} |1 + t(0, x_2)z + s(0, x_2)z^2| = \min_{|z| \leq 1} |1 - 2x_2z|^2 > 0$ . In other words, the roots of the equation  $1 + tz + sz^2$  lie outside the unit disk ( $|z| \leq 1$ ) when  $-x_2 = 1/2, x_1 = 0$ . For an arbitrary point  $(x_1^*, x_2^*)$  that satisfies  $0 < -x_2^* < 1, 0 < x_1^* < 1$ , we may connect it to the point  $(0, 1/2)$  with a line segment. It is obvious that the two roots of  $1 + t(x_1, x_2)z + s(x_1, x_2)z^2$  vary continuously as  $(x_1, x_2)$  moves along this line segment. The orbits of the two roots must be two continuous paths

in the complex plane in the process mentioned above, and each of them begins with a point outside the unit disk and cannot end up with a point inside the unit disk unless it hits the unit circle ( $|z| = 1$ ) some time. However, neither root can hit the unit circle because it is true that  $\min_{0 \leq \theta < 2\pi} |1 + t(x_1, x_2)e^{i\theta} + s(x_1, x_2)e^{2i\theta}| = (1 + x_2)^2(1 - x_1^2) / \sqrt{a(x_1, x_2)} > 0$ . Therefore, both roots of the equation  $1 + t(x_1^*, x_2^*)z + s(x_1^*, x_2^*)z^2$  should lie outside the unit disk. This completes the proof of  $I_2(x_1, x_2) = 2\pi \log a(x_1, x_2)$  ( $0 < -x_2 < 1, 0 < x_1 < 1$ ), and the generalization to  $x_2 = 0$  or  $x_1 = 0$  case is a trivial calculation.

■  
It can be verified by simple algebra that Eqn. (A31) gives the free energy expression that is exactly equivalent to Eqn. (12). This circuitous approach provides an independent method to evaluate the partition function in the 1D atom chain.

† Present Address: Department of Chemistry and Chemical Biology, Harvard University, Cambridge, MA 02138, USA.

‡ To whom correspondence should be addressed. Email: xfjin@fudan.ac.cn

- 
- <sup>1</sup> F. A. Lindemann, Phys. Zeit. **11**, 609 (1910)  
J. J. Gilvarry, Phys. Rev. **102**, 308 (1956)
- <sup>2</sup> M. Born, J. Chem. Phys. **7**, 591 (1939)
- <sup>3</sup> E. Grüneisen, Ann. d. Physik (4) **39**, 257 (1912)
- <sup>4</sup> W. Braunbeck, Zeits. f. Physik **38**, 549 (1926)
- <sup>5</sup> N. v. Raschevsky, Zeits. f. Physik **40**, 214 (1927)
- <sup>6</sup> K. Herzfeld and M. Goepfert-Mayer, Phys. Rev. **46**, 995 (1934)
- <sup>7</sup> J. E. Lennard-Jones and A. F. Devonshire, Proc. Roy. Soc. A **169**, 317 (1939); **170**, 464 (1939)
- <sup>8</sup> G. Grimvall and S. Sjödin, Physica Scripta, **10**, 340 (1974)
- <sup>9</sup> J. L. Tallon, Phil. Mag. A **39**, 151 (1978)
- <sup>10</sup> Z. H. Jin, P. Gumbsch, K. Lu and E. Ma, Phys. Rev. Lett. **87**, 055703 (2001)
- <sup>11</sup> A. Tryanov and E. Tosatti, Phys. Rev. B, **38**, 6961 (1988); R. Ohnesorge, H. Löwen and H. Wagner, Phys. Rev. E, **50**, 4801 (1994); J. Q. Broughton and G. H. Gilmer, J. Chem. Phys. **79**, 5095 (1983); **79**, 5105 (1983)
- <sup>12</sup> M. I. Baskes, Phys. Rev. Lett. **83**, 2592 (1999)
- <sup>13</sup> V. Halpern, J. Phys.:Condens. Matter **12**, 4303 (2000)
- <sup>14</sup> N. Sandberg, B. Magyari-Köpe, and T. R. Mattsson, Phys. Rev. Lett. **89**, 065901 (2002)
- <sup>15</sup> K. Nordlund and R. S. Averback, Phys. Rev. Lett. **80**, 4201 (1998)
- <sup>16</sup> A. Bongiorno, L. Colombo, F. Cargnoni, C. Gatti and M. Rosati, Europhys. Lett., **50**, 608 (2000)
- <sup>17</sup> S. Birner, J. P. Goss and R. Jones, P. R. Bridson, S. Öberg, *Proceedings of ENDEASD* (Stockholm 2000)
- <sup>18</sup> J. I. Landman and C. G. Morgan, J. T. Schick, P. Papoulias and A. Kumar, Phys. Rev. B **55**, 15 581 (1997)
- <sup>19</sup> K. W. Ingle, R. C. Perrin and H. R. Schober, J. Phys. F: Metal Phys, **11**, 1161 (1981)
- <sup>20</sup> F. H. Stillinger and T. A. Weber, J. Chem. Phys. **81**, 5095 (1984)
- <sup>21</sup> J. Cardy, J. Phys. A: Math. Gen. **29**, 1897 (1996)
- <sup>22</sup> A. V. Granato, Phys. Rev. Lett. **68**, 974 (1992)
- <sup>23</sup> C. N. Yang and T. D. Lee, Phys. Rev. **87**, 404 (1957); T. D. Lee and C. N. Yang, Phys. Rev. **87**, 410 (1957).
- <sup>24</sup> R. K. Pathria, *Statistical Mechanics*, 2nd ed., Elsevier (Singapore) Pte Ltd, 2001
- <sup>25</sup> Kerson Huang, *Introduction to Statistical Physics*, Taylor & Francis, 2001
- <sup>26</sup> A. F. Barabanov and V. M. Berezovskii, Zh. Eksp. Teor. Fiz. **106**, 1156 (1994); H. Rosner, R. Hayn and J. Schulenburg, Phys. Rev. B **57**, 13660 (1998); J. Richter, A. Voigt, J. Schulenburg, N. B. Ivanoc and R. Hayn, J. Magn. Magn. Mat. **177-181**, 737 (1998)
- <sup>27</sup> B. M. McCoy and T. T. Wu, *The Two-dimensional Ising Model*, Harvard University Press, Cambridge, Massachusetts, 1973
- <sup>28</sup> N. Goldenfeld, *Lectures on Phase Transitions and the Renormalization Group* (Addison Wesley, 1992)
- <sup>29</sup> For  $\langle \sigma_k \sigma_{k+1} \rangle \rightarrow -1$ ,  $J_1 > 0$  is a necessary condition. When  $J_1 < 0$ ,  $\langle \sigma_k \sigma_{k+2} \rangle$  is still continuous at 0K.
- <sup>30</sup> It should be mentioned here that in 3D case, near the melting point, we could only expect  $J_1 > J_2$  and  $J_2 < 0$ , but could no longer suppose that  $J_1 > 0$ . This is because (1) at finite temperature,  $J_1 > J_2$  is already sufficient to guarantee that NNN atom pairs are more stable than NN atom pairs; (2) experimental results about the Frenkel defect formation energy in fcc metals are  $(6J_1 - 12J_2) \approx 4 \sim 5\text{eV}$ , while the bonding energy  $-J_2 = 0.5 \sim 1\text{eV}$ , so the  $J_1 < 0$  case will be inevitable while modelling a realistic solid in three dimensions.
- <sup>31</sup> Fortunately, most exact results in this paper do not change when  $J_1$  is replaced by  $-J_1$ , for instance,  $F_{\text{conf}}$ ,  $S_{\text{conf}}$ ,  $\langle \sigma_k \sigma_{k+2} \rangle$ ,  $\partial c / \partial T \dots$ , but  $\langle \sigma_k \sigma_{k+1} \rangle$  and  $(\partial S_{\text{conf}} / \partial J_1)_{J_2, T}$  always bear the same sign as  $-J_1$ . For a negative NN pair energy  $J_1$ , the correlation length (represented by  $\mu(J_1, J_2, T)$ ) equals the one (represented by  $\lambda(|J_1|, J_2, T)$ ) for positive NN pair energy  $|J_1|$ . However, the form of the correlation functions are generally different for positive and negative NN pair energies,  $\partial \mu(J_1, J_2, T) / \partial |J_1| = \partial \lambda(|J_1|, J_2, T) / \partial |J_1|$ .
- <sup>32</sup> R. E. Peierls, Ann. Inst. Henri Poincaré **5**, 177
- <sup>33</sup> M. Kac and J. C. Ward, Phys. Rev. **88**, 1332
- <sup>34</sup> N. V. Vdovichenko, Soviet Physics JETP **21**, 350 (1965)
- <sup>35</sup> L. D. Landau and E. M. Lifshitz, *Statistical Mechanics, Part I* (Butterworth-Heinemann, 1999)
- <sup>36</sup> Since each oblique edge that links a lattice site to an interstitiality site changes the parity of the site label, a closed diagram should include an even number of oblique edges. Therefore, the power of  $x_1$  should be an even number for the diagram contribution to be non-zero. That is why the partition function is invariant under the transformation  $J_1 \mapsto -J_1$ .
- <sup>37</sup> This result can be indeed generalized rigorously to all diagrams, including those with “repeated-bonds”.